ORIGINAL ARTICLE

Investigation of the microstructure evolution and mechanical properties of a TC6 alloy blade preform produced by cross wedge rolling

Junling Li[1] · Baoyu Wang[1] · Shuang Fang[2] · Ping Chen[1]

Abstract

Cross wedge rolling (CWR) is one of the most effective plastic deformation methods utilized for the production of shaft parts or non-shaft preforms with refined grains and improved mechanical properties. The main goal of this work was to study the influence of CWR process parameters on the microstructure evolution and mechanical properties of a TC6 alloy and determine the suitable process parameters for a TC6 alloy blade preform fabricated with CWR. The results showed that the volume fraction of the equiaxed α phase (f_{α_e}) decreased from ~0.38 to ~0.04 by increasing the initial deformation temperature, and the elongation (El) also decreased from ~19.6 to ~11.8% because dislocation slip first started in the equiaxed grains and then dispersed into the adjacent grains. Thus, additional equiaxed grains contributed to an increased plasticity. Moreover, with an increasing area reduction, the value of f_{α_e} increased from ~0.14 to ~0.31, and the grain refinement and microstructure uniformity also increased. In addition, the El was significantly reduced by over 50%, but the ultimate tensile strength (UTS) and yield strength (YS) increased under WC (water cooling) conditions due to the precipitation of the acicular secondary α phase and pinning effect of the small equiaxed α phase. Based on the determined suitable parameters, the TC6 alloy blade preform was successfully manufactured by CWR, the microstructure was evenly distributed, and the UTS, YS and El were 1120.1 MPa, 1020.9 MPa and 15.2%, respectively, which meet the current technical requirements.

Keywords TC6 titanium alloy · Cross wedge rolling · Microstructure evolution · Mechanical properties · Blade preform

1 Introduction

Titanium and titanium alloys are highly valued and widely used in the aerospace, petroleum and chemical industries due to their excellent specific strength, high operating temperature and corrosion resistance. TC6 is a two-phase titanium alloy that can withstand a working temperature up to 450 °C. Therefore, it is preferentially used in the production of compressor discs, drums and other parts, especially blades in aero-engines [1]. To achieve better mechanical properties, high-temperature plastic deformation processes are commonly used to manufacture aero-engine blades, such as forging [2–4]. Multiple steps are sequentially required and collaborated in the production of the blades, and heading/extrusion or free forging are used for preliminary shape-forming. Considering the structure inheritance, the microstructure and mechanical properties of a preform directly affect the serviceability of the resulting blade; therefore, the production of blade preforms is of importance. During extrusion, due to the long time and large contact area between the billet and mould, an excessive amount of deformation heat is not easy to dissipate, affects the deformed microstructure of the billet and deteriorates the contact surface of the mould [5]. Moreover, free forging relies on manual operation, and the process parameters are not easy to accurately control. The TC6 alloy has strong temperature and strain rate sensitivities, which worsens the situation. Therefore, a cross wedge rolling (CWR) process was proposed to manufacture a preform for a titanium alloy blade.

Cross wedge rolling is one of the most effective plastic deformation methods that is utilized for the production

✉ Junling Li
junlingli@ustb.edu.cn

1   School of Mechanical Engineering, University of Science and Technology Beijing, No.30 Xueyuan Road, Haidian District, Beijing 100083, China

2   Beijing Institute of Aeronautical Materials, Beijing 100095, China

of shaft parts with refined grains and improved mechanical properties, such as high-speed railway axles and hollow valves [6, 7]. Moreover, it also has the characteristics of high forming efficiency, environmental protection and strong structural stability, which can effectively compensate for the shortcomings of the current blade preforming process, and experience has suggested that CWR can be used for the production of preforms, such as crankshafts and hip implants [8, 9].

For two-phase titanium alloys, the phase composition and morphology are significantly influenced by thermo-mechanical processing (TMP) parameters and cooling methods [10–12], and a substantial research has been carried out on this method. Xu et al. [13] investigated the microstructure evolution of a Ti-17 alloy with a lamellar colony structure during isothermal forging (IF), and the results showed that the length of the lamellar alpha phase decreased with strain and deformation temperature, but the thickness was independent of the strain. The results by Ansarian et al. [14] showed that the mean grain size can be significantly reduced from 64 to 1 μm by 6 passes during multi directional forging (MDF). Multi-isothermal direction forging (MDIF) was also applied to produce Ti–6Al–4V alloys. A homogeneous microstructure with a grain size of approximately 0.5 μm was achieved, and it exhibited a high ultimate tensile strength (UTS) and yield strength (YS) of 1190 MPa and 1170 MPa, respectively, as well as a good elongation (El) of 10.4% [15]. In contrast to the above studies, CWR is a non-isothermal continuous severe plastic deformation thermo-mechanical process. As the rolls rotate continuously, the billet undergoes periodic radial and axial deformation, which induces a series of metallurgical processes, such as dislocation motion, dynamic and static recovery, and dynamic and static recrystallization, leading to changes in the phase composition, morphology and mechanical properties [16–18]. However, there are few studies on the influence of CWR parameters on the microstructure evolution and mechanical properties of titanium alloys in the currently available research.

Accordingly, the present work aims to investigate the microstructure evolution and mechanical properties of a TC6 alloy during the CWR process, and the underlying mechanism for the impact of the phase composition and morphology on the mechanical properties was analysed. Based on this foundation, the suitable process parameters for a TC6 alloy during CWR processing were determined and used to guide the practical production of blade preforms. Moreover, the microstructure and tensile properties of the TC6 blade preform at room temperature were tested.

2 Materials and experimental procedures

2.1 Materials

The material used in this work was a TC6 alloy whose initial microstructure mainly consisted of a strip-like α phase and a couple of equiaxed α phase and a couple of equiaxed phases dispersed throughout the matrix, as shown in Fig. 1. The beta transus temperature was 985 °C via the metallographic method, and the details of the experiment are in a previous work [19].

2.2 Experimental procedures

To investigate the influence of the process parameters on the microstructure of the TC6 alloy during CWR, experiments under different process conditions were carried out. In a previous study, the influence of all the process parameters was investigated, and the results showed that mould parameters, including the forming angle and stretching angle, are non-significant influencing factors [20]. Therefore, the initial deformation temperature (IDF), area reduction and cooling methods were studied. In this paper, the IDFs varied from 850 °C to 930 °C with an interval of 20 °C; the area reduction was 20%, 30%, 40%, 50% and 60%; and the cooling methods were water cooling (WC) and air cooling (AC). The studied process parameters are shown in Table 1.

A corresponding finite element (FE) model was established to provide the supporting analysis, such as the distribution of the strain and instantaneous temperature. Figure 2 shows the geometric model used for the FE simulation that includes CWR rolls, guide plates and billets. To ensure the correctness of the simulation results, the strain–stress curves obtained from the isothermal compression were imported into the software material library, and the boundary
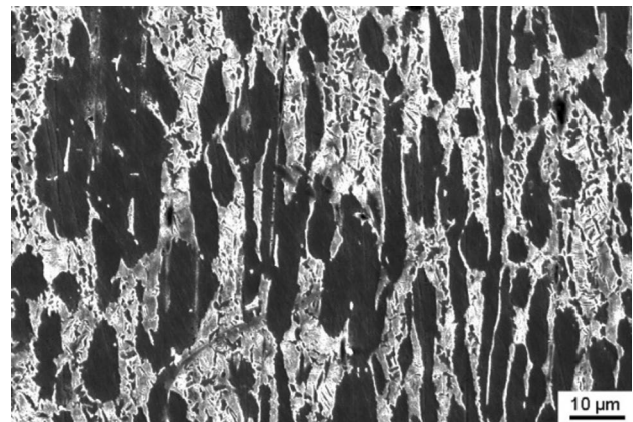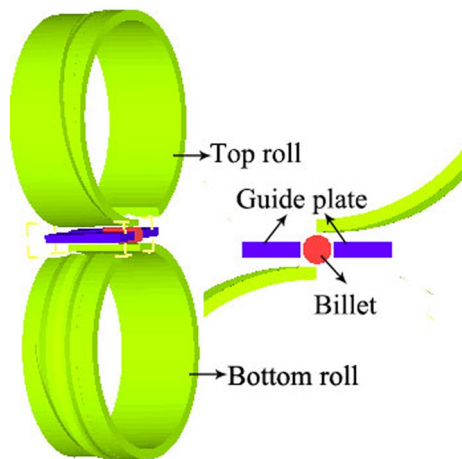

Fig. 1 The initial microstructure of the as-received TC6 alloy

Table 1 The detailed process parameters

Serial no.	IDF/°C	Area reduction	Cooling method
1	850, 870, 890, 910, 930	50%	AC
2	890	20%, 30%, 40%, 50%, 60%	AC
3	870, 930	50%	WC, AC

Fig. 2 Geometric model of the CWR process

Table 2 The parameters used in the FE simulation

Parameter	Value
Forming angle of tools (°)	25
Stretching angle of tools (°)	7.5
Tools temperature (°C)	20
Tools speed (r m^{-1})	8
Friction coefficient	0.9
Convection coefficient between ambient air and billet (W m^{-1} K^{-1})	20
Contact heat transfer coefficient between the tools and billet (kW m^{-2} K^{-1})	10

conditions were set as in the previous research, which was verified [20]. Specifically, half of the geometrical model was used to define the symmetry boundary, all parts were defined as rigid bodies except for the billet, and a shear model was used to model the friction between the contact bodies. The simulation parameters were identical to those of the cross wedge rolling experiments, and other parameters are shown in Table 2.

After being rolled, the TC6 parts were cut into symmetrical sections along the axial direction. Optical microscopy (OM) and scanning electron microscopy (SEM) were performed at room temperature to observe the microstructure. The sample preparation for OM and SEM included mechanical grinding and polishing with a fine abrasive and then chemical etching with Kroll's solution. The values of f_{α_e} were quantitatively measured by Image Pro-plus software. Standard tensile tests at room temperature were carried out according to GB/T 228.1-2010 to evaluate the mechanical properties, and the samples were taken along the axial direction at the core of the TC6 rolled parts.

3 Results and discussion

3.1 Effect of the initial deformation temperature

Figure 3 shows the deformed microstructure under different IDFs for an area reduction of 50% and AC. It is obvious that the deformed microstructure contained an equiaxed α phase of different sizes, and the values of f_{α_e} decreased with increasing IDF, as shown by the quantitative results in Fig. 4d. When the IDF was lower than 890 °C, the value of f_{α_e} slightly reduced, but the total content was higher than 0.3. However, when the IDF was higher than 900 °C, the value of f_{α_e} showed a sharp decline, especially when the IDF was 930 °C. In this paper, the transition from a slight to sharp decline seemed to be earlier than that in isothermal compression because CWR is a non-isothermal deformation method, and the deformation temperature rise was converted from the intense plastic deformation, leading to a higher instantaneous temperature and accelerating the phase transformation process.

In the deformed microstructure, the platelet α phase and residual beta phase comprised the structure of the β transformation. When the rolled parts were cooled from a high temperature in $\alpha + \beta$ two-phase or β single-phase regions, martensite decomposition occurred, and after nucleation and growth, the platelet α phase was formed. From Fig. 3, it can be seen that when the IDF was relatively low, for example, at 850 °C, the platelet α phase was very small without clear boundaries. However, as the IDF increased, the platelet α phase began to grow and merged into the coarse α phase, as shown in Fig. 3e. This is because the martensitic transformation is a thermal activation process, and insufficient driving forces are generated at low temperatures. Conversely, high temperatures provide enough driving force and lead to a substantial amount of nucleation and fast growth.

The grain boundary α phase, also called the intergranular α phase, is usually found on the original grain boundaries, as shown in Fig. 3d, e. It is obvious that the grain boundary α phase was discontinuous initially. However, the grain boundary α phase became thick and continuous at an IDF of 930 °C, which means that the instantaneous temperature exceeded the beta transus temperature. Figure 5 shows the
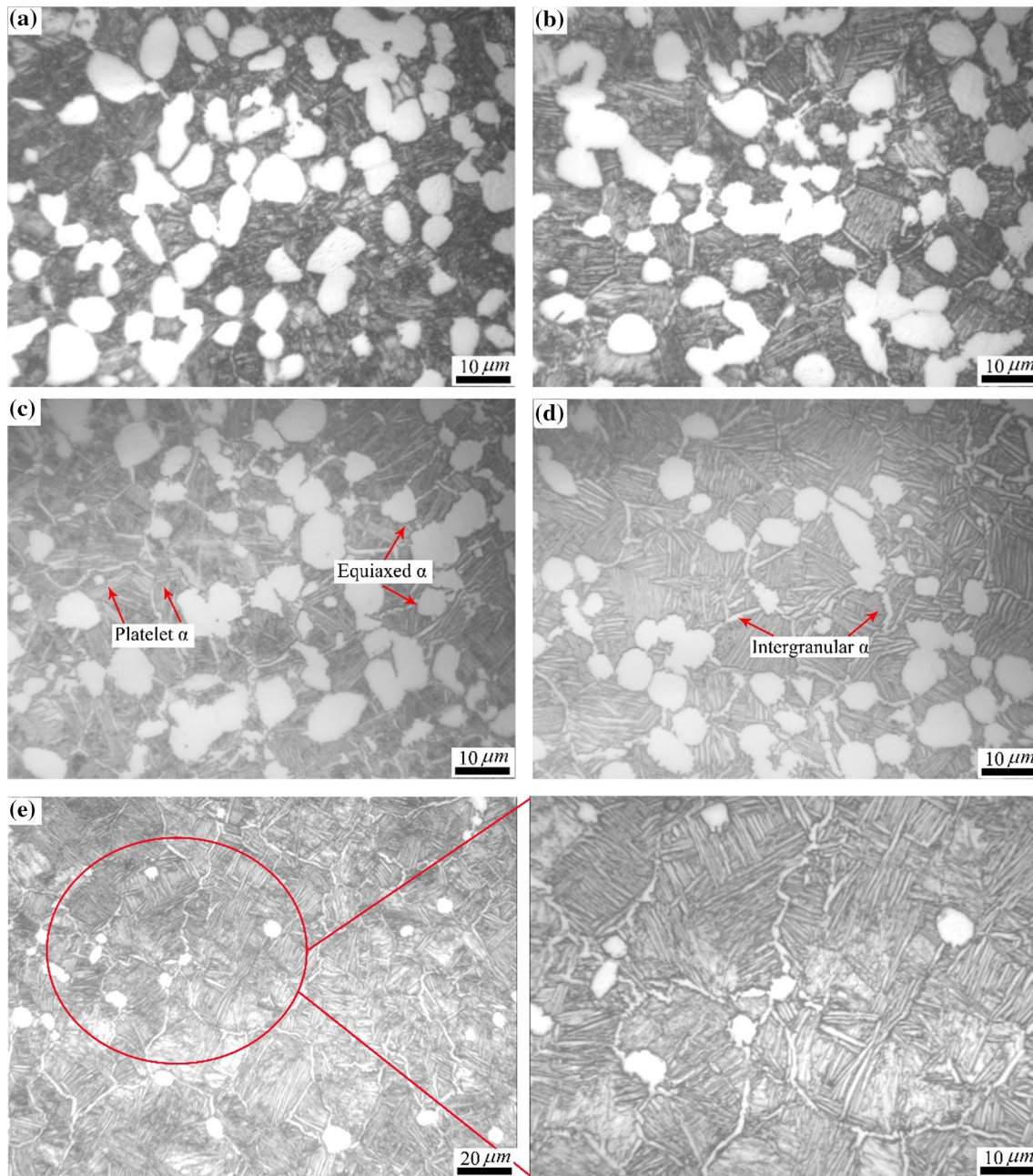
Fig. 3 Effect of the IDF on the microstructure of the rolled TC6 parts for an area reduction of 50% and upon AC: **a** 850 °C, **b** 870 °C, **c** 890 °C, **d** 910 °C and **e** 930 °C

instantaneous temperature distribution of the TC6 rolled parts extracted from the FE simulation under IDFs of 890 °C and 930 °C, which confirms the deduction above.

Figure 4 shows a comparison of the mechanical properties of rolled TC6 parts at different IDFs. Generally, there is an inverse relation between the El and strength characteristics. Specifically, the IDFs can be divided into two regions based on the variation tendency. In the range from 850 to 890 °C, the changes in all the mechanical properties were negligible. However, a sharp change appeared at an IDF of

930 °C, where the El significantly decreased to 11.8% and the UTS and YS increased. In addition, the El decreased upon increasing the IDF, which is consistent with the f_{α_e} values. This is because tensile deformation involves the proliferation, movement and annihilation of dislocations, and dislocation proliferation is inclined to be generated in the equiaxed α phase. When subjected to plastic deformation, dislocation slip first starts in equiaxed grains with the largest orientation factor and then disperses into adjacent grains to avoid stress concentrations and ductile fracture;
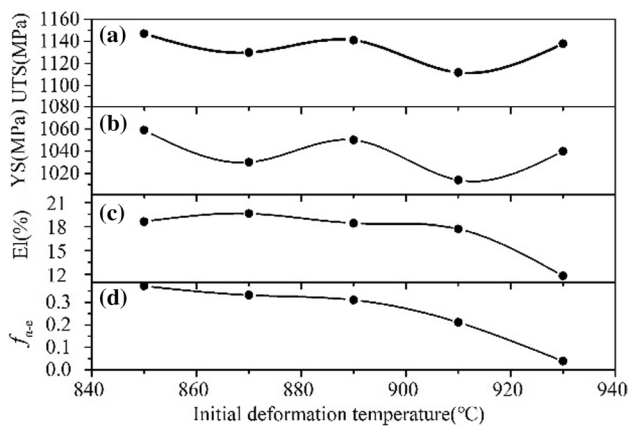
Fig. 4 Comparison of the mechanical properties for different IDFs: **a** UTS, **b** YS, **c** El and **d** f_{α_e}

therefore, equiaxed grains contribute to an improved plasticity [21]. For the microstructure at an IDF of 930 °C, there were very few equiaxed α phases scattered in the structure that experienced the β transformation, and the platelet α phase was short, slender and intertwined. When this α phase was coupled with the continuous intergranular α phase, the strength properties were improved, but the El trend was the opposite of this. Therefore, in terms of tensile properties, IDF improved for the TC6 alloy parts during CWR below 910 °C.

3.2 Effect of the area reduction

Figure 6 represents the effect of the area reduction on the microstructure of rolled TC6 parts at an IDF of 890 °C and for AC. It was observed that the value of f_{α_e} increased by increasing the area reduction, but the growth slowly increased and stayed flat. The value of f_{α_e} was approximately 0.15 at an area reduction of 20%, as shown in Fig. 7. However, the El was almost equal to those under other conditions, which can be attributed to the coarse and relatively independent α platelet phase. The orderly independent platelet α phase can reduce the slip resistance and improve
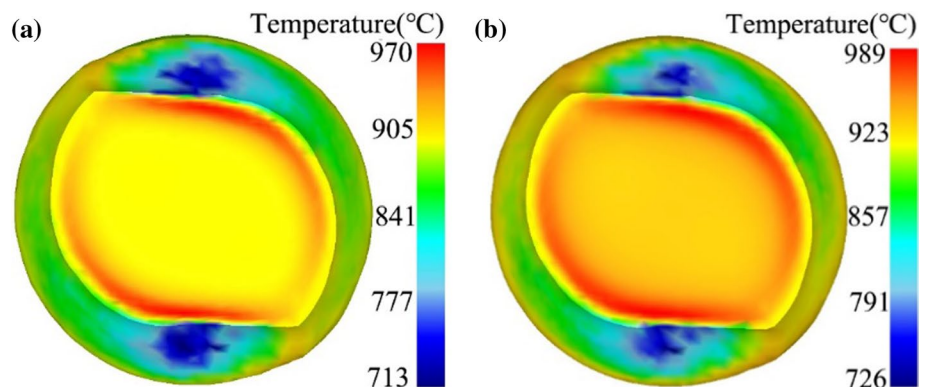
the plasticity, similar to the contribution of the equiaxed α phase. However, the coarse platelet α phase impairs the strength properties, resulting in poor comprehensive properties [22]. With an increase in the area reduction, the coarse platelet α phase was severely distorted and crushed into short and slender pieces with blurry boundaries [21]. Moreover, the strength properties decreased after reaching a summit. In Fig. 7, it can be seen that a larger area reduction was not conducive to an improvement in the mechanical properties.

During the CWR process, the area reduction is an indicator of the degree of plastic deformation. With the goal of ensuring that additional deformation defects, such as necking and fracture, are not formed, and a large area reduction is conducive to grain refinement. The deformed microstructures at different positions on the symmetrical cross section under area reductions of 20% and 30% are shown in Figs. 8 and 9, respectively. Three points were distributed along the radial direction and are referred to as from the core, middle and edge. Compared with Fig. 8a, the platelet α phase was relatively short and scattered in Fig. 8c because plastic deformation was mainly experienced by the local material at the edge and hardly penetrated into the core material when the degree of deformation was small. Figure 10a shows that the total strain decreased inward from the edge, and it was too small to be ignored in the centre of the billet. However, the non-uniform plastic deformation can be improved by increasing the area reduction up to 30%, as shown in Fig. 9. The long platelet and grain boundaries were crushed and blurred, and the fine equiaxed α phase was indistinguishably dispersed throughout the cross section. What can be inferred from the results is that the grains can be further refined, and the uniformity can be improved, by increasing the area reduction. For a TC6 alloy during CWR, the minimum lower limit should not be less than ~30%.

3.3 Effect of the cooling method

The effect of the cooling method on the deformed microstructure at IDFs of 870 °C and 930 °C is presented in Fig. 11. It is evident that the cooling method had a
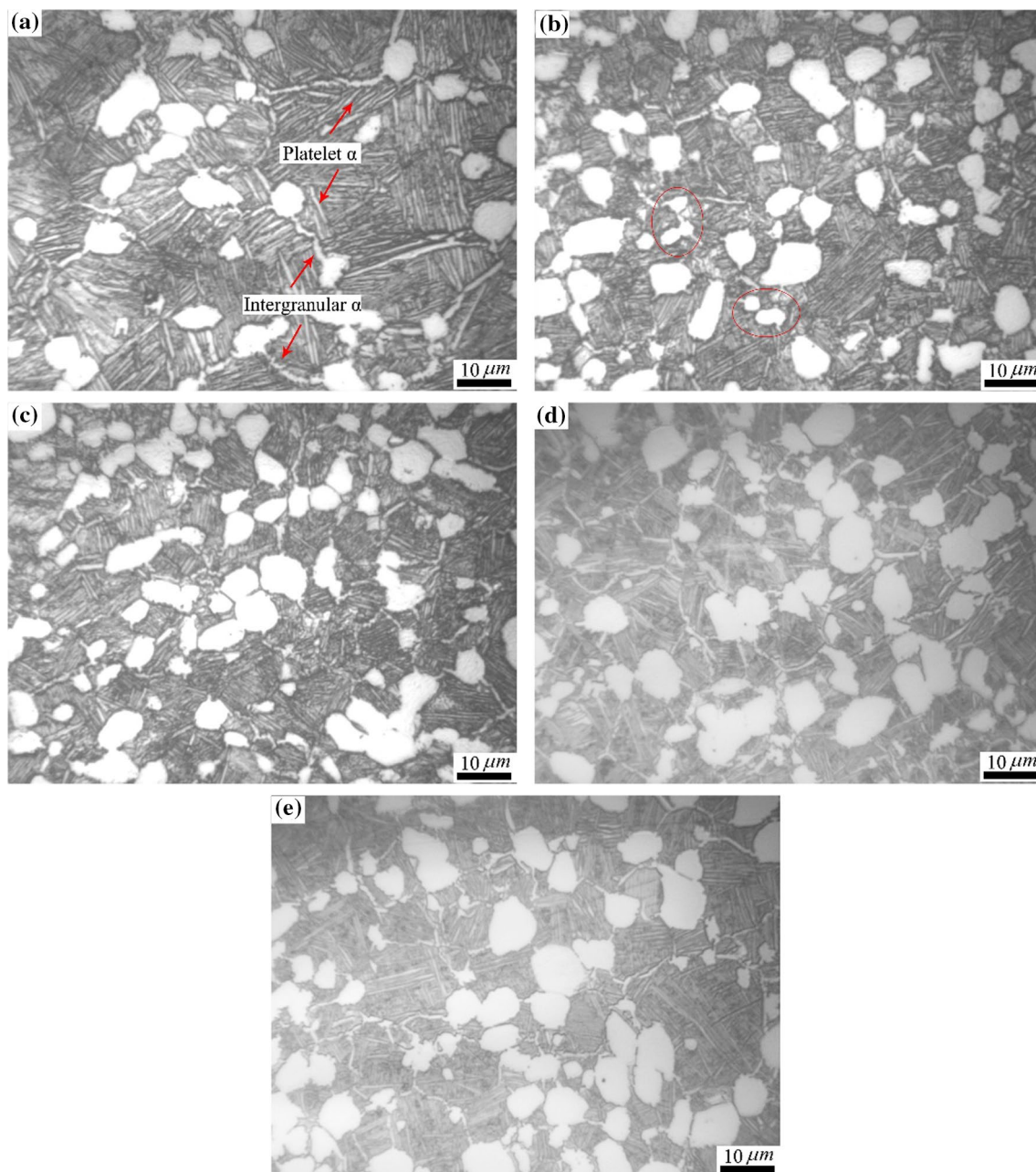
Fig. 5 The instantaneous temperature distribution of rolled TC6 parts at different IDFs: **a** 890 °C and **b** 930 °C

Fig. 6 Effect of the area reduction on the microstructure of rolled TC6 parts at an IDF of 890 °C and upon AC: **a** 20%, **b** 30%, **c** 40%, **d** 50% and **e** 60%

remarkable influence for the studied IDFs. Under WC conditions, there was only a secondary α phase instead of a transformed β phase due to rapid decomposition of the martensite and extreme subcooling; the acicular α phase was regular, closely arranged and formed colony in the original β phase boundaries [11]. This type of α phase resisted fatigue crack growth and improved the strength but significantly reduced the plastic ductility, as shown in Fig. 12. Another important factor responsible for the poor ductility was the small equiaxed α phase under WC conditions due to the limited

growing time. However, some of the equiaxed α phase was located on the original β phase boundaries, resulting in the phase boundaries that were bent outward. This equiaxed α phase had a pinning effect on the boundaries, hindering phase boundary slip and excessive growth. Compared with the mechanical properties under AC conditions, the El was significantly reduced, but the strength properties behaved in the opposite way. Therefore, the WC after plastic deformation played a role in the work hardening of the TC6 rolled
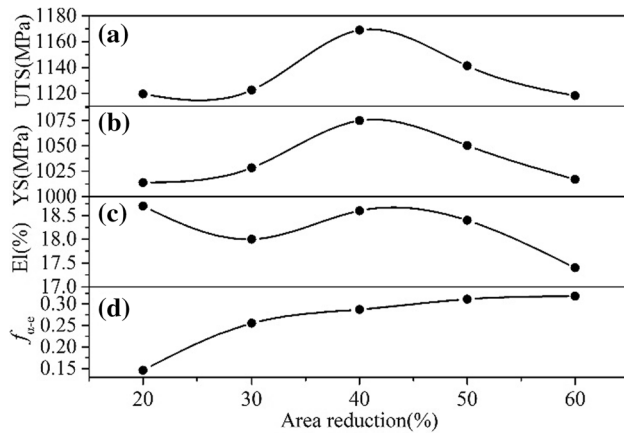
Fig. 7 Comparison of mechanical properties for different area reductions: **a** UTS, **b** YS, **c** El and **d** f_{α_e}

parts; if additional plastic deformation is required, fast cooling methods, such as WC, should be avoided.

4 Application

Based on the investigation results of the microstructure evolution of a TC6 alloy during the CWR process, suitable parameters were determined. Using the CWR process to fabricate blade preforms made of a TC6 alloy that has excellent mechanical properties is an innovative challenge but can be overcome. According to the requirements for compressor blades used in aero-engines, a reasonable blade preform was designed and successfully fabricated by the CWR process. Billets with initial dimensions of φ45 mm were rolled at an IDF of 890 °C and then air-cooled to room temperature. The deformed microstructure of the cross section at different positions along the axial direction is shown in Fig. 13. It is obvious that the microstructure consisted of an equiaxed α phase, platelet α phase and residual β phase. Moreover, the phase morphology and content of the deformed microstructure at three
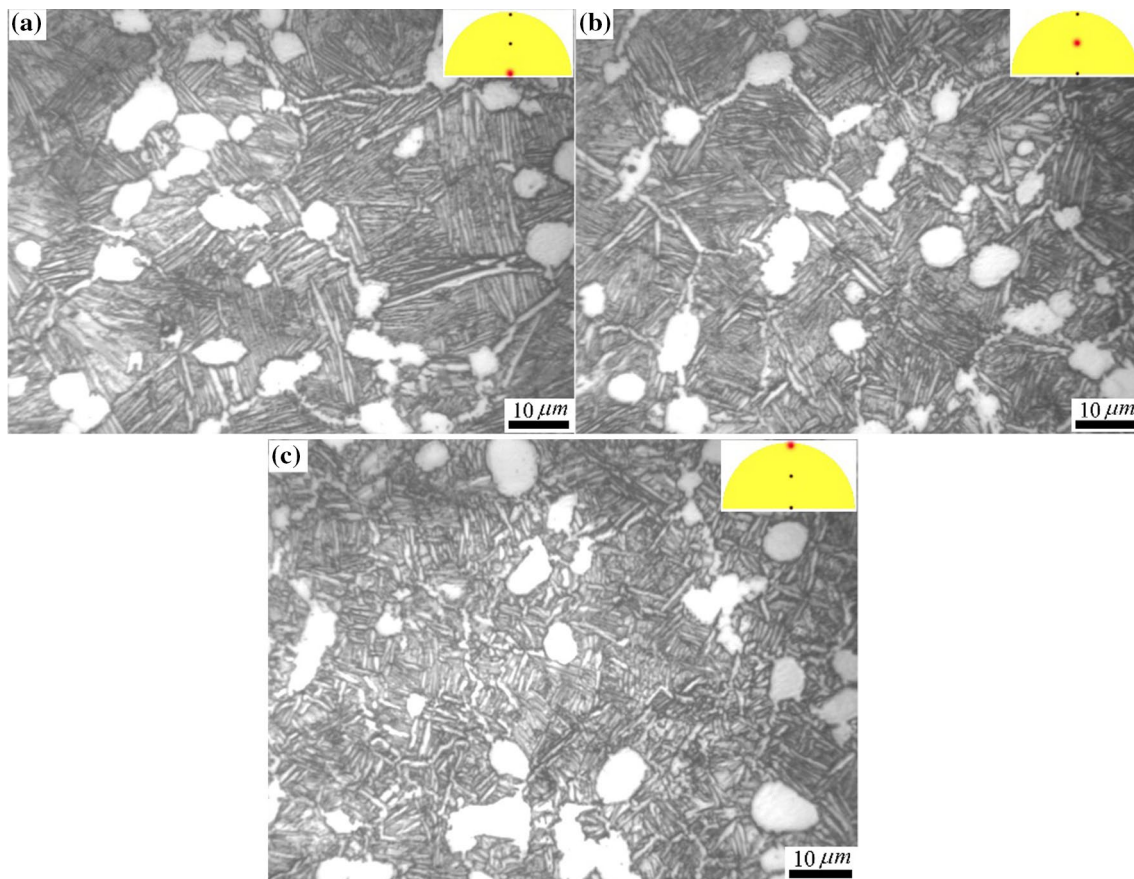

Fig. 8 The deformed microstructure for an area reduction of 20% at different positions on the symmetrical cross section: **a** core, **b** middle and **c** edge
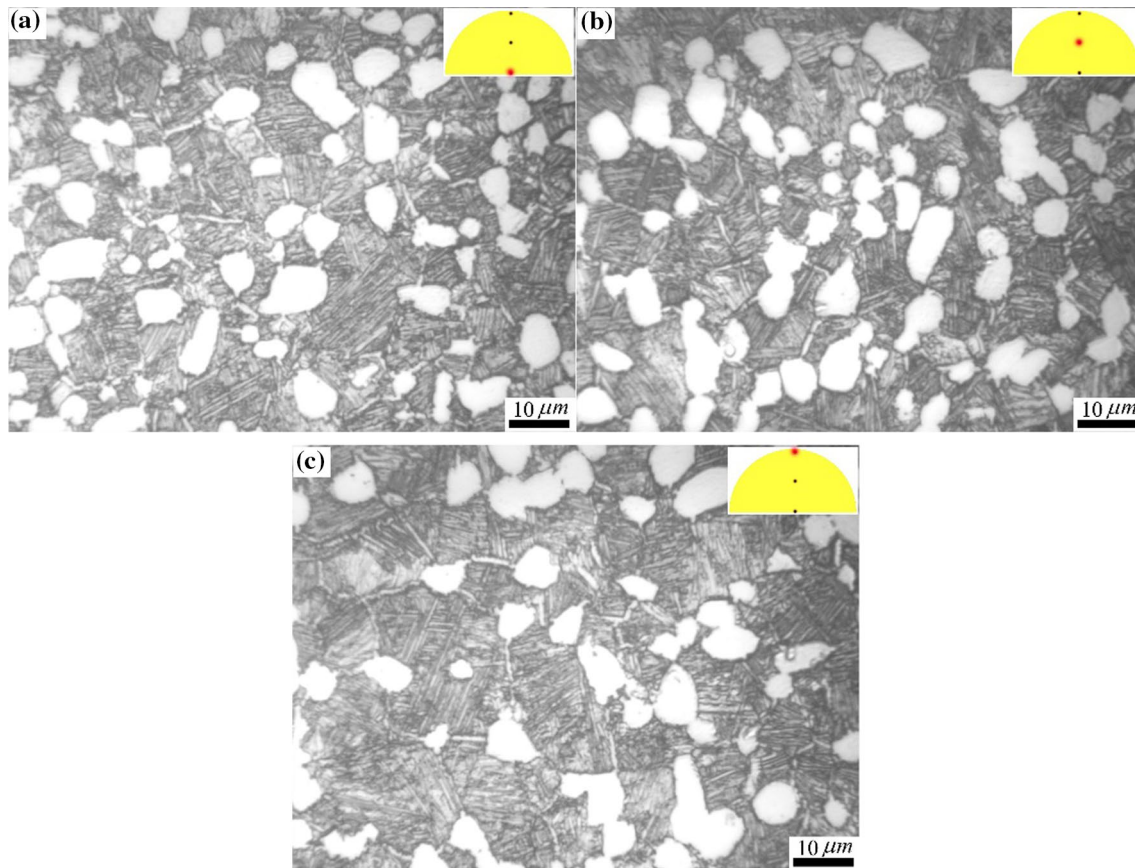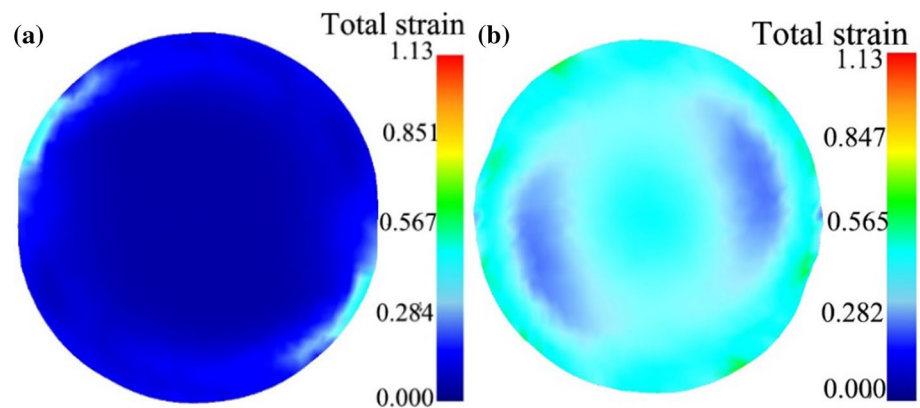
Fig. 9 The deformed microstructure for an area reduction of 30% at different positions on the symmetrical cross section: **a** core, **b** middle and **c** edge

Fig. 10 The total strain distribution of the rolled TC6 parts under different area reductions: **a** 20% and **b** 30%

different locations on the same cross section were identical, as shown in Table 3, which indicates that the entire cross section of the material was involved in the deformation. Nevertheless, there were additional and smaller equiaxed α phases dispersed throughout the microstructure on the edge. Tensile samples from the core of the rolled parts were prepared to test their mechanical properties, and the results showed that the UTS, YS and El were 1120.1 MPa, 1020.9 and 15.2%, respectively. Currently, the technical index requires the UTS and EI to be higher than 1030 MPa
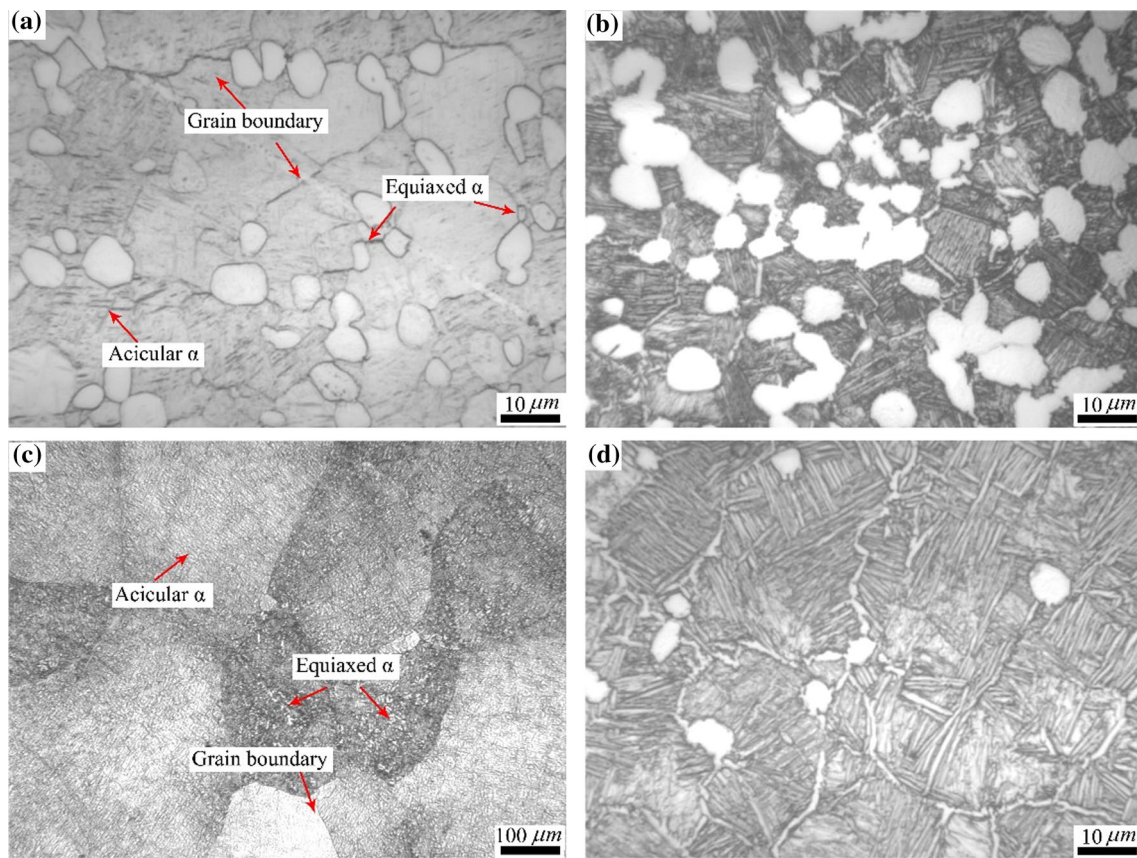
Fig. 11 Effect of the cooling method on the microstructure of the rolled TC6 parts at an IDF of 870 °C with **a** WC and **b** AC; and at an IDF of 930 °C with: **c** WC and **d** AC
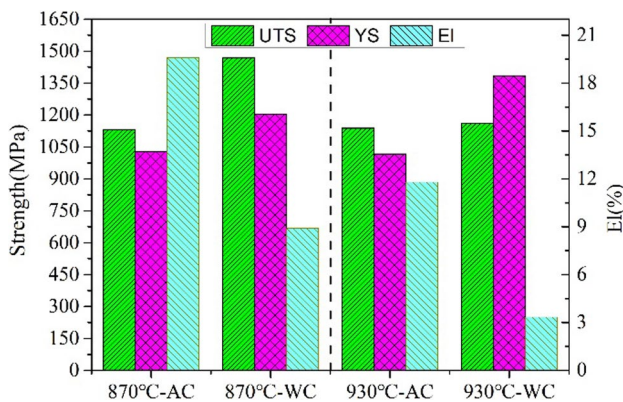

Fig. 12 Comparison of the mechanical properties at IDFs of 870 °C and 930 °C for different cooling methods

and 8%, respectively. Therefore, the tensile properties of the TC6 alloy blade preform fully meet the current technical requirements.

5 Conclusions

1. The deformed microstructure consisted of equiaxed and platelet α phases and residual β phase, and the platelet α phase began to grow and merged into the coarse phase upon increasing the IDF under AC conditions due to thermal activation. Moreover, the El decreased from ~19.6 to ~11.8% by increasing the IDF, which is consistent with the variation trend for the f_{α_e} from ~0.38 to ~0.04. This is because the dislocation slip first started in the equiaxed grain and then dispersed into adjacent grains, so additional equiaxed grains contribute
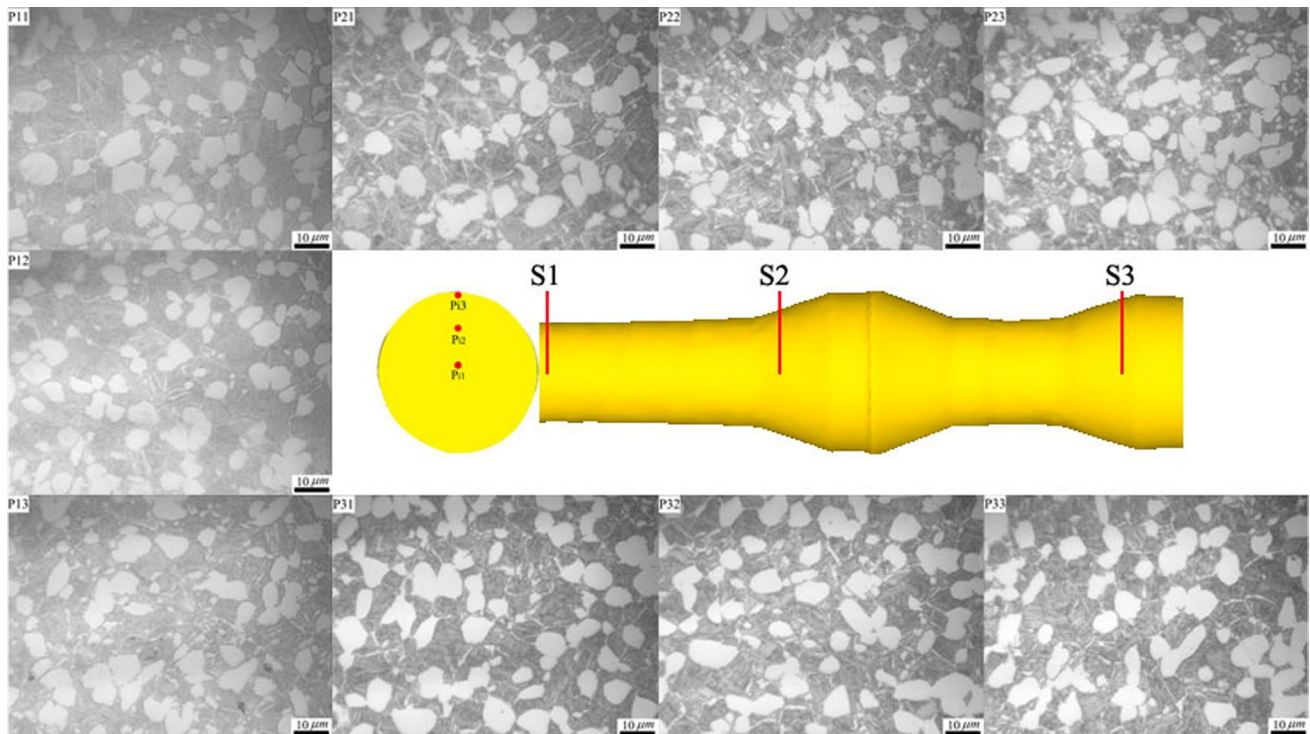
Fig. 13 Microstructure of the TC6 alloy blade preformed by the CWR process

Table 3 The values of f_{α_e} at different points

Point	f_{α_e}	Point	f_{α_e}	Point	f_{α_e}
P11	0.307	P21	0.311	P31	0.318
P12	0.313	P22	0.320	P32	0.312
P13	0.311	P23	0.322	P33	0.310

improve the plasticity. However, the intertwined platelet α phase and continuous intergranular α phase improved the strength properties when the IDF increased up to 930 °C. To obtain excellent comprehensive properties, the IDF of TC6 alloy parts during CWR improves at temperatures lower than 910 °C.

2. By increasing the area reduction, the values of f_{α_e} increased from ~0.14 to 0.31, and the grain refinement and microstructure uniformity also increased. However, there was no remarkable difference in the El, but the strength properties first increased and then decreased. The essential reason is that the coarse and relatively independent platelet α phase, which was not completely fractured in the lower area reduction, reduced the slip resistance, similar to the equiaxed α phase. For the TC6 alloy during CWR, the minimum lower limit of area reduction should not be less than ~30%.

3. Under WC conditions, the El was significantly decreased by over 50%, but the strength properties increased due to the precipitation of the acicular secondary α phase and pinning effect of the smaller equiaxed α phase. If further plastic deformation is required, fast cooling methods should be avoided.

4. Based on the determined suitable parameters, the TC6 alloy blade preform was successfully manufactured by the CWR process, and the results demonstrated that the microstructure was evenly distributed with values of f_{α_e} higher than 0.3. The UTS, YS and El were 1120.1 MPa, 1020.9 MPa and 15.2%, respectively, which meet the current technical requirements.

References

1. Leyens C, Peters M. Titanium and titanium alloys: fundamentals and Applications. 1st ed. Darmstadt: betz-druck GmbH; 2003.
2. Huang SH, Zong YY, Shan DB. Application of thermohydrogen processing to Ti6Al4V alloy blade isothermal forging. Mater Sci Eng, A. 2013;561:17–25.
3. Liu YL, Du K, Zhan M, Yang H, Zhang FW. Physical modeling of blade forging. J Mater Process Technol. 2000;99:141–4.

4. Na YS, Yeom JT, Park NK, Lee JY. Prediction of microstructure evolution during high temperature blade forging of a Ni–Fe based superalloy, alloy 718. Met Mater Int. 2003;9:15–9.

5. Painter B, Shivpuri R, Altan T. Prediction of die wear during hot-extrusion of engine valves. J Mater Process Technol. 1996;59:132–43.

6. Huo YM, Bai Q, Wang BY, Lin JG, Zhou J. A new application of unified constitutive equations for cross wedge rolling of a high-speed railway axle steel. J Mater Process Technol. 2015;223:274–83.

7. Ji HC, Liu JP, Wang BY, Zhang ZR, Zhang T, Hu ZH. Numerical analysis and experiment on cross wedge rolling and forging for engine valves. J Mater Process Technol. 2015;221:233–42.

8. Meyer M, Stonis M, Behrens BA. Cross wedge rolling and bi-directional forging of preforms for crankshafts. Prod Eng Res Dev. 2015;9:61–71.

9. Behrens BA, Stonis M, Blohm T, Richter J. Investigating the effects of cross wedge rolling preforming operation and die forging with flash brakes on forging titanium hip implants. Int J Mater Form. 2018;11:67–76.

10. Qin DY, Guo DZ, Zheng L, Li YL. Dynamic recrystallization of Ti-5553 alloy during sub-transus thermomechanical processing: mechanisms and its role in formation of a bi-modal structure. J Alloy Compd. 2018;769:725–31.

11. Julien R, Velay V, Vidal V, Dahan Y, Forestier R. Characterization and modeling of forged Ti–6Al–4V Titanium alloy with microstructural considerations during quenching process. Int J Mech Sci. 2018;142–143:456–67.

12. Shi ZF, Guo HZ, Liu R, Wang XC, Yao ZK. Microstructure and mechanical properties of TC21 titanium alloy by near-isothermal forging. Trans Nonferr Met Soc. 2015;25:72–9.

13. Xu JW, Zeng WD, Sun X, Jia ZQ. Microstructure evolution during isothermal forging and subsequent heat treatment of Ti-17 alloy with a lamellar colony structure. J Alloy Compd. 2015;637:449–55.

14. Ansarian I, Shaeri MH, Ebrahimi M, Minarik P, Bartha K. Microstructure evolution and mechanical behaviour of severely deformed pure titanium through multi directional forging. J Alloy Compd. 2019;776:83–95.

15. Zhang ZX, Qu SJ, Feng AH, Hu X, Shen J. Microstructural mechanisms during multidirectional isothermal forging of as-cast Ti–6Al–4V alloy with an initial lamellar microstructure. J Alloy Compd. 2019;773:277–87.

16. Huo YM, Lin JG, Bai Q, Wang BY, Tang XF, Ji HC. Prediction of microstructure and ductile damage of a high-speed railway axle steel during cross wedge rolling. J Mater Process Technol. 2017;239:359–69.

17. Wang MT, Li XT, Du FS, Zheng YZ. A coupled thermal–mechanical and microstructural simulation of the cross wedge rolling process and experimental verification. Mater Sci Eng A. 2005;391:305–12.

18. Wang MT, Li XT, Du FS, Zheng YZ. Hot deformation of austenite and prediction of microstructure evolution of cross-wedge rolling. Mater Sci Eng A. 2004;379:133–40.

19. Li JL, Wang BY, Hang H, Fang S, Chen P, Shen JX. Unified modelling of the flow behaviour and softening mechanism of a TC6 titanium alloy during hot deformation. J Alloy Compd. 2018;748:1031–43.

20. Li JL, Wang BY, Qi Y, Fang S, Huang X, Chen P. Investigating the effect of the process parameters on the cross wedge rolling of TC6 alloy based on the temperature and strain rate sensitivities. Int J Adv Manuf Technol. 2019;103:2563–77.

21. Yang XM, Zhao ZL, Ning YQ, Guo HZ, Li H, Yuan SC, Xin SW. Microstructural evolution and mechanical property of isothermally forged BT25y titanium alloy with different double-annealing processes. Mater Sci Eng A. 2019;745:240–51.

22. Abbasi SM, Momeni A. Effect of hot working and post-deformation heat treatment on microstructure and tensile properties of Ti–6Al–4V alloy. Trans Nonferr Met Soc. 2011;21:1728–34.